JMEPEG (2009) 18:369–377
DOI: 10.1007/s11665-008-9300-y

1059-9495/$19.00

Roles of Surface Booster System on Bending of Thin-Walled Copper Tube

Ding Tang, Dayong Li, Zhongwei Yin, and Yinghong Peng

(Submitted October 24, 2007; in revised form July 26, 2008)

Thin-walled C12200 circular copper tube has been widely used in HVAC (heating, ventilation, air conditioning, and refrigeration) industry. Rotary draw bending is a versatile and precise method in forming of thin-walled copper tubes. Wall thinning and sectional fattening are the two main defects that affect tube quality in industrial applications. With traditional die settings, such as adjusting position or type of the mandrel, one factor usually decreases at the expense of increasing the other. An assistant equipment, surface booster system, has been recently developed to relieve both defects at the same time. In the present study, the role of the booster system in the bending process is investigated with finite element simulation. A basic model of copper tube rotary draw bending is established and validated by experiments. Then, cases of different sets of main parameters of the booster system are studied. The relationship between loading force, lower displacement, speed of the booster, and forming characteristics of tube is obtained based on which suggestions about process parameters settings are given. The results provide a better understanding of the role of the booster system in the improvement of forming quality.

Keywords copper tube, finite element modeling, rotary draw bending, surface booster system

1. Introduction

Circular copper tubes have been widely used in cooling and heating systems,such as ACR (air conditioning/refrigeration) tube and heat pipe for water heater (Ref 1). Among the different methods of copper tube bending, rotary draw bending is the most versatile, cost-effective, and precise method for thin-walled tubes (Ref 2). Figure 1 shows the basic dies used in rotary draw bending. In bending of C12200 circular tubes, over wall thinning and sectional shape degradation occur easily. Figure 2 shows the defects of sectional shape degradation formed with the method of rotary draw bending. As ACR tubes work under large internal pressure, these defects reduce the strength at the elbow region and shorten its service life (Ref 3, 4). Defects of sectional shape degradation disturb the flow inside the tube.

To improve the forming quality of rotary draw bending, many scholars have carried out researches on the tool set such as die closing and axial feeding. Stachowicz (Ref 1) used analytical method to study the changes of wall thickness of the outside with and without upsetting when using both the simple and special mandrels. Li (Ref 5) has studied the ball-and-socket mandrel and examined the effects of geometry parameters of shank and balls. Peng and Tang (Ref 6) have studied the roles of the mandrel types and compared the effect of three main types of mandrel on the forming qualities. However, for the two main defects of wall thinning and shape degradation, the conventional tool settings decreases one factor at the expense of increasing the other (Ref 5, 6). Generally, work is done to find a point where both defects are within certain acceptable extent under free wrinkling condition.

Surface booster system is a new technique which improves forming quality of tube rotary draw bending by changing movement style of the pressure die. For normal equipment of the rotary draw bending equipment without booster system, there are two kinds of pressure dies, static and traveling type. Static pressure die does not move. Traveling pressure die, also called follower pressure die, can reduce galling and marking of the tube by alleviating some drag during bending. Surface booster system uses pressure die with active motions. So, it can alleviate both the defects of shape degradation and over wall thinning at the same time by improving the metal flow condition during the bending process.

Figure 3 shows the scheme of a draw bending equipment with a kind of booster system, which is composed of a normal rotary draw bending equipment and a pressure die booster and control system. Apparently, the booster system can be divided into driving device (for movement along the tube axis) and a vertical pressure adjustment device (for movement perpendicular to the tube axis). In Fig. 3, both movements are hydraulic power driven. In practice, there are two main methods to add pressure to the tube. One is using hydraulic cylinder with a flexible joint, which leaves the pressure die with little tolerance of self-adjustment for a better contact with the tube, and the other is to apply a rigid displacement to the pressure die by a lead-screw system with rigid joint. Both methods have been discussed in this study.

During the bending process, hydraulic cylinder (#1) slides to apply a pressing force on the tube. Hydraulic cylinder (#2) slides the pressure die, which applies a friction force on the

Ding Tang, Dayong Li, Zhongwei Yin, and **Yinghong Peng**, School of Mechanical Engineering, Shanghai Jiao Tong University, Shanghai 200030, China. Contact e-mail: dyli@sjtu.edu.cn.

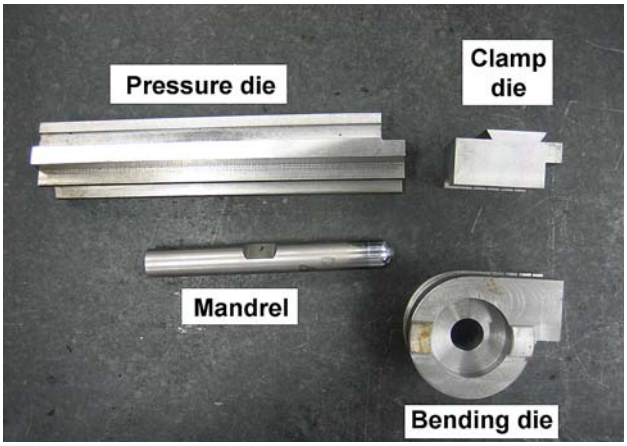

Fig. 1 Dies of rotary draw bending equipped with surface booster system

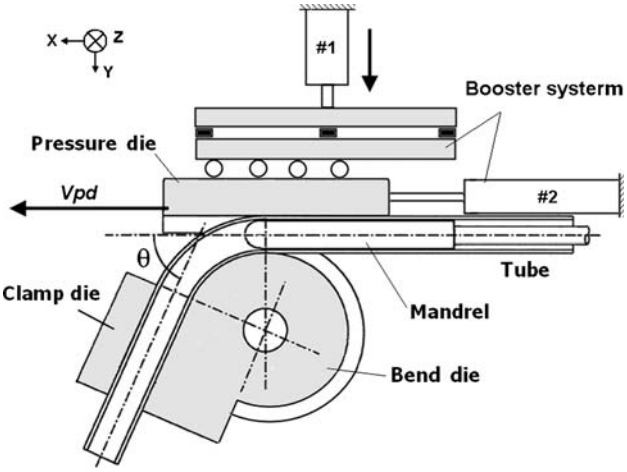

Fig. 3 The schematic of rotary draw bending equipment with surface booster system

Fig. 2 Defects of rotary draw bending

surface of the tube. Then, as the tube is pulled around the rotary bending die, the pressure die moves forward with a certain speed, which generates a horizontal booster force to the upper surface on the tube.

Up to now, few papers have dealt with the roles of a surface booster system. In this study, surface booster processing has been investigated with both FE method and experiment. A typical type of C12200 ACR tube with a diameter of 20 mm (widely used in HVAC industry) is used as the object of study. A FE model of the bending process with surface booster effect has been established and validated with experiments. The two types of pressing force methods, which are named flexible force loading and rigid displacement loading, have been compared. The two main processing parameters of the surface booster system, pressing force and booster speed, and their effects on the quality of forming have been investigated.

2. Material Properties of C12200

The performance of tube material C12200 for heat transfer and brazing is outstanding; however, up to now, studies about its forming process are still not available. Friction and mechanical properties are important boundary and computational conditions for FE simulation. In this section, both properties are tested with experiments.

2.1 Friction Property

As surface booster system works with friction force between pressure die and tube, friction property is specially focused on. In a tube bending process, there are five contact interfaces between tube and dies: tube/mandrel, tube/wiper die, tube/bend die, tube/clamp die, and tube/pressure die. Because the plastic deformation zone concentrates on the bending part, which is not in contact with die, and most of tube parts that contacts with die still belong to nondeformation zone, namely rigid zone, the classical Coulomb model has been chosen to represent the interfaces friction condition:

$$\sigma_f = \mu\sigma_n$$

where σ_f is the frictional stress, μ the friction coefficient, and σ_n the stress on the contact surface.

Pin-on-Disc experiment for calculating the friction coefficient has been carried out between C12200 material of the tube and die steel, CrWMn. This test was performed according to ASTM standards (ASTM 1943). Friction tests were carried out at sliding speeds of 0.2 m s^{-1} under the load of 100 to 300 N. The test duration was 1 min for each specimen. The specimens of the Pin-on-Disc test and their installation on the test machine

Fig. 4 Disc-pin test for measuring friction coefficient

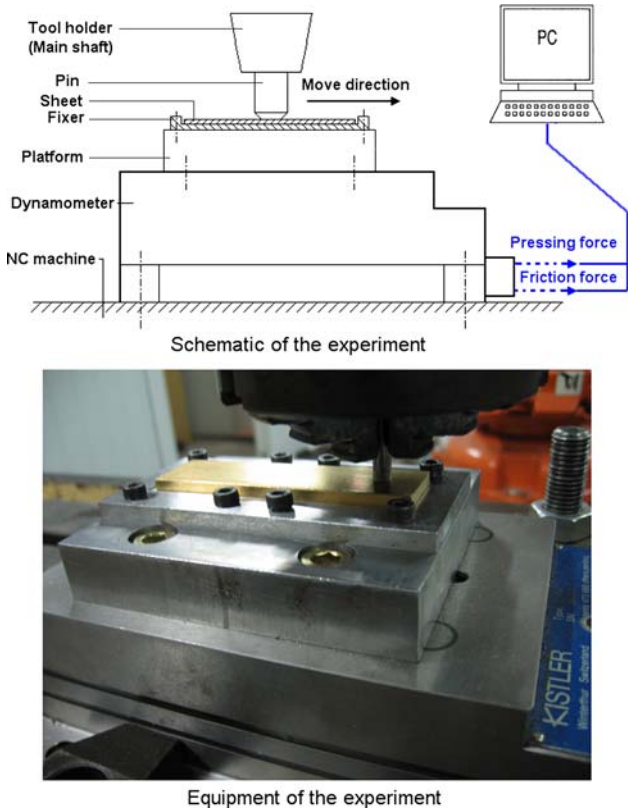

Fig. 5 Experiment for measuring friction coefficient

are shown in Fig. 4. Tests were performed on both groups of steel pin with copper disc and copper pin with steel disc.

By post-processing the collected data, the average value of coefficient of friction is considered as 0.071.

The result of the Pin-on-Disc experiment is basically reliable, but the accuracy is not high enough. Because the relative movement between pin and disc is not smooth, results have large run-out error. Furthermore, the specimen gets heated up before the numerical results become stable. Therefore, an effective, accurate, and convenient experiment for measuring the friction coefficient has been designed (already applied for a patent) and carried out.

As shown in Fig. 5, a high accuracy Kistler dynamometer with three channels (for three directions of force with sensitivity of 10 mv/N) is fixed on the worktable of the NC machine. Sheet specimen with the material of the tube is fixed upon the platform of the dynamometer, while the pin specimen with the material of the tools is held with the main shaft of the NC machine. Before the relative movement, the main shaft of the NC machine goes down, which makes the pin specimen attach on the surface of the sheet specimen vertically. This place will be recorded as the original coordinate of the main shaft. As the main shaft is adjusted to go down with displacement from 0 to 0.18 mm, different pressing forces on the sheet specimen can be gained.

The worktable moves with the speed of 6 m/min along the horizontal axis. The Kistler sensor under the specimen will output the voltage signals of vertical and frictional force of the whole movement process to a computer through an amplifier. As the friction coefficient is the ratio of the two voltage signals, so the calibration error of each force is avoided.

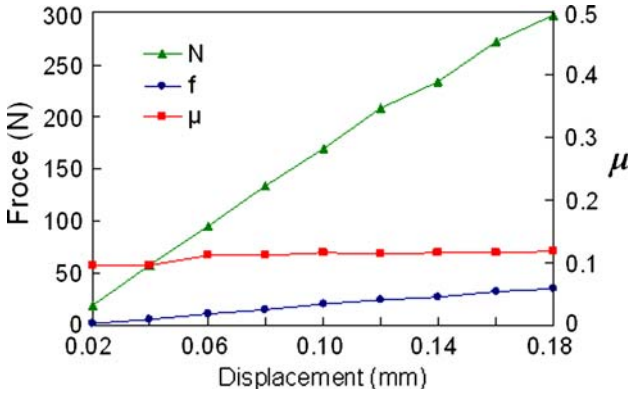

Fig. 6 Result of a specimen with pin-sheet test

Figure 6 shows the result of a specimen with pin-sheet test. As the pressing force increased, the friction coefficient remains stable on the whole. By post-processing the collected data, the average value of coefficient of friction is considered to be 0.11 ± 0.02. Compared to the result of the traditional pin-disc test, it is believed that the pin-sheet method is more accurate, so the value of 0.11 is considered to be the coefficient of friction between the tube and the die steel.

2.2 Mechanical Property

In FE simulation, the dies are modeled with rigid parts. So, only the property of the tube is needed. To obtain the mechanical properties of the tube, C12200, a tensile material

Fig. 7 Specimen damaged in material test

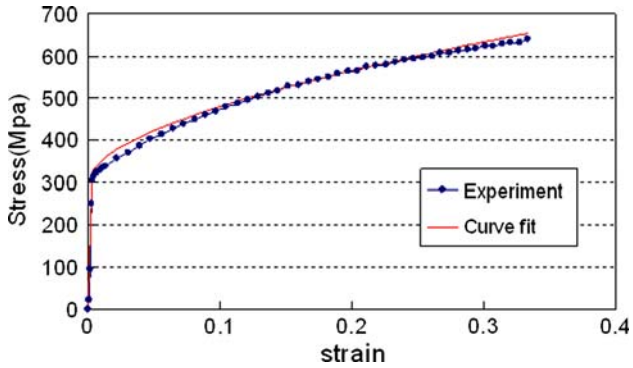

Fig. 8 Stress-strain diagram from the material test

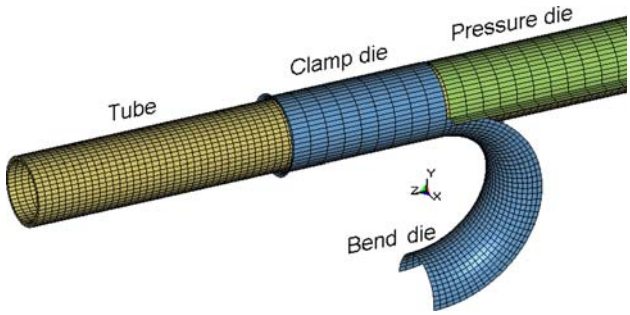

Fig. 9 Finite element model for the bending simulation

Table 1 Common geometry parameters

Geometry parameters	Value, mm
Bend radius	31
Tube outer diameter	20
Wall thickness	1
Tube length	310

Table 2 Design of geometry parameters

Geometry parameters	Value
Lower displacement (for displacement loadings model)	0 mm, 0.2 mm, 0.4 mm
Pressing force (for force loadings model)	500 N, 1000 N, 3000 N, 5000 N
Booster speed (for force loadings model, 3000 N)	$1.05V_{tan}$, $1.2V_{tan}$, $1.3V_{tan}$, $1.5V_{tan}$, $1.7V_{tan}$

test has been performed. A Special clamper has been designed for the tube specimen. The specimen disabled during the test is shown in Fig. 7. The constitutive equation representing the material behavior was obtained through the Marquardt's curve fitting method. Figure 8 shows the stress-strain relation.

Its constitutive equation is:

$$\sigma_e = E\varepsilon \quad \text{(Eq 1)}$$

$$\sigma_p = K(\varepsilon_e + \varepsilon_p)^n \quad \text{(Eq 2)}$$

where E is the Young's modulus (112 GPa), K the strength coefficient (654.76 MPa), ε_e the offset elastic strain (0.31%), n the strain-hardening exponent (0.57), and ε_p is the effective plastic strain.

3. FE Modeling

The finite element modeling on the tube bending process includes the following content: tool and die geometries, boundary constraints, surface interactions, and material properties.

In this study, the explicit dynamic finite element code LS-DYNA has been applied in FEM modeling of the rotary tube bending process.

3.1 Geometry Settings and Parameters Design

The geometry and finite element modeling of tube bending process is shown in Fig. 9 with the initial tubular blank and tool set. The tools are represented as rigid bodies. The tubular blank is represented by four-node shell elements. Geometry parameters are shown in Table 1.

For the two loading methods, in FE simulation, lead-screw system with rigid joint is represented by applying a rigid displacement to the pressure die along the direction perpendicular to the axis of the tube. For method using hydraulic cylinder and flexible joint, a force perpendicular to the axis of the tube is applied to the pressure die. Displacement and pressing force applied on the pressure die, as well as booster speed, are all parameterized. For the friction force to act on the tube by the pressure die in right direction, the velocity of the pressure die, V_{pd}, should be higher than the tangential velocity of the metal flow on the surface of the tube, V_{tan}. Therefore V_{pd} is represented as multiple of the V_{tan}. Table 2 shows design of the parameters.

3.2 Dynamic Boundary Condition

According to different contact conditions, the friction coefficient can be classified into two kinds: normal and 'Rough,' in which 'Rough' type refers to no relative slipping when nodes contact each other and is suitable for the tube/clamp die friction conditions. For normal contact condition, result of pin-sheet friction test is applied. The contact interfaces between the tube and the dies are defined with the 'Surface-to-surface contact' option. According to the condition of tight

clamping of the clamp die, the sliding is not allowed between the contact surfaces.

Curves with trapezoidal profile are used to define the smooth angular/translate velocity of the bend die, the clamp die, and the pressure die. The 'Velocity Curves' applied to the dies act as the boundary constraints and loadings. The bending time needed is 2 s at the bending speed of π/4 rad/s. Both bend die and clamp die are constrained to rotate about the global *Z*-axis, while the pressure die is constrained to translate only along the global *X*-axis with the same linear speed as the centerline bending speed of the bend die.

3.3 Validation by Experiments

To evaluate FE result of thicknesses distribution of bent tubes, bent tube was cut with a wire electrical discharge machine (WEDM), and the thickness of the cross section was measured with a precision of 0.01 mm (Fig. 10). The tube is taken from the experiment of rotary draw bending with booster system. The booster speed is $1.05V_{\tan}$ and pressure force is 500 N. Figure 11 and 12 show the experimental results of wall thickness compared to the FE results of extrados and terminus sides, respectively.

It is found obviously that simulation results share the same trend with the one in the experimental data: thickness of the inner side increases sharply to a plateau, while for outside, it varies much more evenly. The comparison indicates that difference between the simulation and experiment results is also less than 5%. So, the stability and the accuracy of the FE model are validated.

4. Results and Discussion

4.1 Methods of Adding Pressure Force

For the method displacement prescription in FE model, pressure die is set to press on the tube with rigid displacement in *Y*-axis, while for force loading, pressing force is directly loaded on the pressure die and the die is free in the *X*-*Y* plane. Simulation result indicates that contact status of the two methods is quite different.

Figure 13 shows the stress distribution on the tube during the processing under the condition of loading by force. Stage 1 is the original status; in stage 2, the pressure die presses on the tube. Then, in stage 3, the bending die rotates while the pressure die goes forward with higher acceleration and gives the tube both pressure and friction force, which causes spots of summit contact pressure. In stage 4, the tube is deformed by the

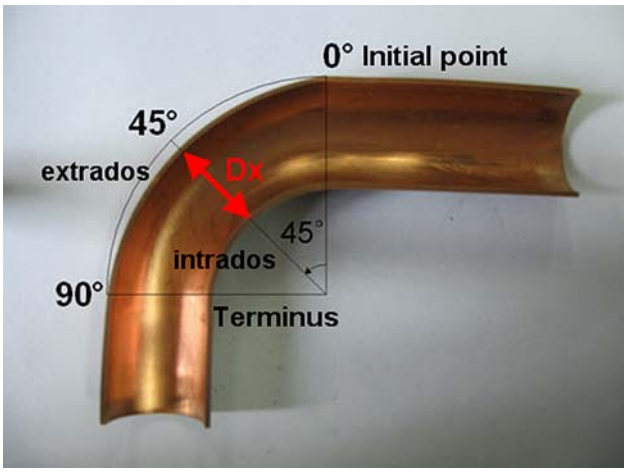

Fig. 10 Method of measuring the cut tube

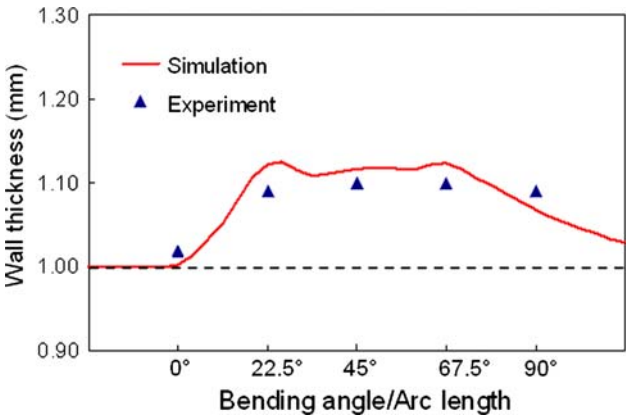

Fig. 11 Wall thickness of inner side/intrados

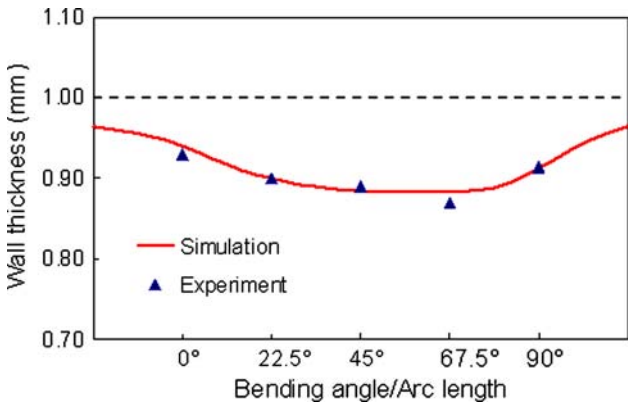

Fig. 12 Wall thickness of outer side/extrados

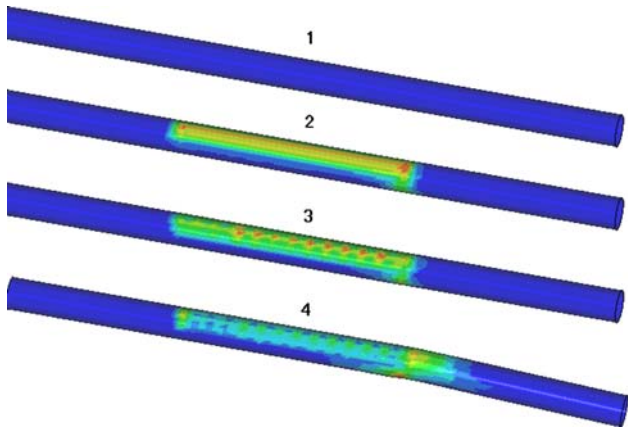

Fig. 13 Effective stress on the tube at the beginning of the process

bending force and the stress caused by bending gradually exceeds the contact pressure.

However, for the displacement loading model, contact area is concentrated at the ends of the pressure die, as shown in Fig. 14. The reason for the unfavorable contact status is mainly the freedom restriction of the pressure die. During the bending process, the rear end and the initial point of the bending part have the trends of uplifting. Meanwhile, the pressing die makes rigid translational motion in *Y*-axis. So the two summit places become the actual contact area.

As surface booster system is to improve the metal flow by surface pushing, obviously the two point contact status cannot give the tube an even and smooth pushing force. Even worse, rigid displacement and bad contact station will cause serious stress convergence, as shown in Fig. 15, which can greatly reduce the forming quality. Therefore, the beneficial range of rigid displacement is very limited and unstable. So, the method of lead-screw system is not qualified for mass production. Between the two kinds of loading modes, the force loading method shows better performance.

4.2 Effect of Pressure Force

To study the variation of wall thinning of each cross section along the bending part, wall thinning degree (ξ) is defined as:

$$\xi = \left|\frac{t_i - t}{t_i}\right| \times 100\% \qquad \text{(Eq 3)}$$

where t_i is initial value of wall thickness and t is wall thickness on a certain point at the cross section.

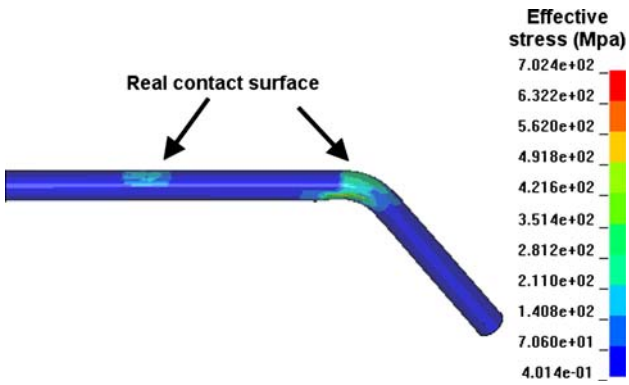

Fig. 14 Real contact surface of displacement loading model

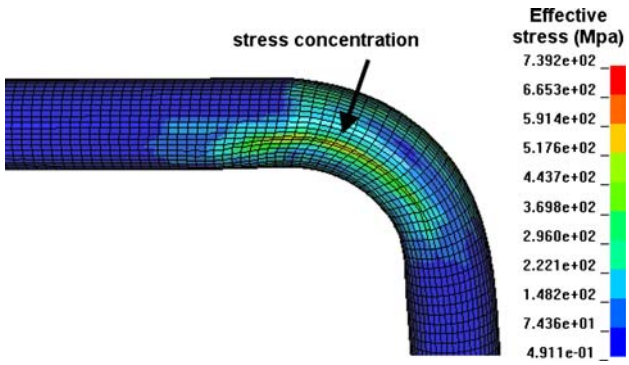

Fig. 15 Stress concentration with displacement loadings model

Figure 16 shows the comparison of ξ along the extrados section of bending part under different pressing forces. With the increase of the loading force from 500 to 5000 N, summit value of wall thinning degree at extrados decreases from 9.15 to 6.02%, which proved that the surface booster system is effective in alleviating the problem of over thinning of tube thickness.

In the intrados of the bending part, ξ represents the increasing of wall thickness. Figure 17 shows the comparison of ξ along the intrados section of bending part under different pressing forces. Compared to Fig. 16, it is seen that the curves are closer to each other, which indicates that without assistant booster effect at local area, ξ does not differ not much. It proves that the effect of the booster system on wall thickness is mainly on the extrados side. For this point, its effect on wrinkling tendency is little.

It is also found that in Fig. 17 the curves still basically share the same trend with curves in Fig. 16: the larger the booster force is, the higher the summit value of wall thinning degree is. It is noted that thickness of tube increases in both sides when surface booster force is larger. The volume of metal at the bending part is increased. So it is concluded that the surface booster system does improve the metal flow by complementing the metal to the bending part from the shank part of the tube, and the complement mainly concentrates at the extrados where it is needed most.

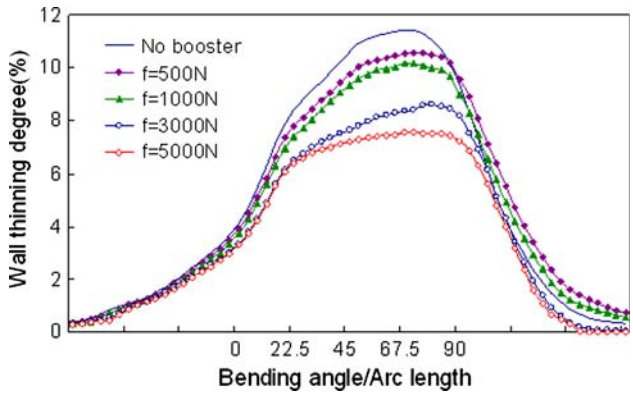

Fig. 16 Reduction of wall thickness at extrados

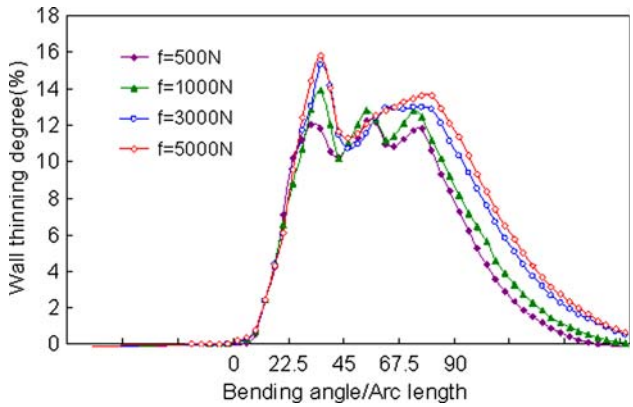

Fig. 17 Increment of wall thinning at intrados

It is known that shape degradation of cross section is another key parameter for forming quality assessment. Shape degradation degree, ψ, other than the ovalization degree, which is able to separate the status of flattening and convex, is defined as follows.

$$\psi = \frac{D_X - D_Y}{D} \times 100\% \quad \text{(Eq 4)}$$

where D_Y is the length of the Y-axis of the elliptic cross section cut by the plane at certain bending angle, as shown in Fig. 18 and D_X is the length of the X-axis perpendicular to corresponding axis of D_Y.

Positive value of ψ means flattening situation while negative means convex situation.

Figure 19 shows the comparison of ψ along the tube bending part, under different pressing forces. With the increase of pressure force on the booster system, summit value of ψ decreases obviously. Under loading of 3000 N, amount of convexity and flattening is almost in average distribution which makes the deformation of tube in a best condition.

Figure 20 shows the effect of pressing force on both wall thickness and sectional shape degradation. The effect of pressing force can be seen clearly: the larger the pressing force is, the better the forming qualities are. ψ_{max} and ξ_{max}, which depict the defect of the forming quality, show linear reduction with the increase of the pressing force; however, when the force exceeds 5000 N, the structure is not steady due to the limitation of booster system stiffness. Also, for the tube, too large a force will cause wall thinning at the part between pressure die and mandrel. Therefore, pressing force between 1000 and 3000 N is the preferable range.

4.3 Effect of Booster Speed

In this section, the effect of booster speed on the forming quality is examined.

Figure 21 shows the varying wall thinning degree, ξ, along the extrados section under different booster speeds from $1.05V_{tan}$ to $1.7V_{tan}$. With the increase of the speed, the degree of wall thinning decreases. As booster speed exceeds $1.3V_{tan}$, its effect on alleviation of wall thinning decreases. From the aspect of the absolute value, booster speed has more influence on ξ than the pressing force does.

Figure 22 shows comparisons of wall thickness factor and sectional shape degradation factor among FE models with different booster speeds. Larger booster speed benefits the forming qualities. The relationship is about exponential descent but when the force exceeds $1.2V_{tan}$, the influence of the factor diminishes. Larger speed of the pressure die will have little effect on quality improvement. Therefore, $1.05V_{tan}$ to $1.2V_{tan}$ is the preferable range.

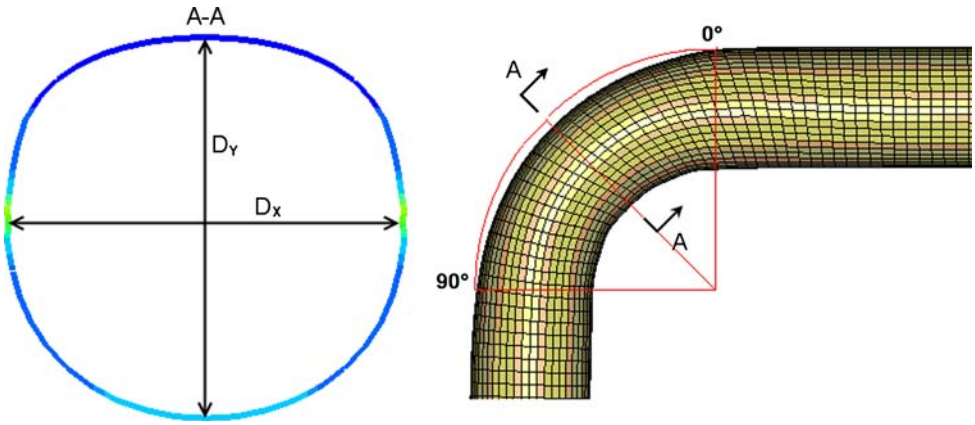

Fig. 18 Definition of parameters accessing the sectional deformation

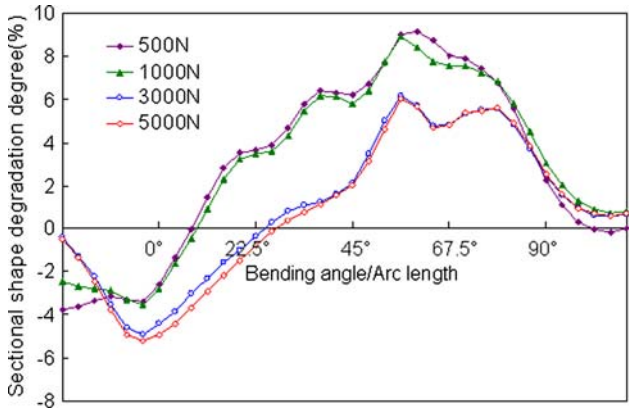

Fig. 19 Comparison of sectional shape degradation

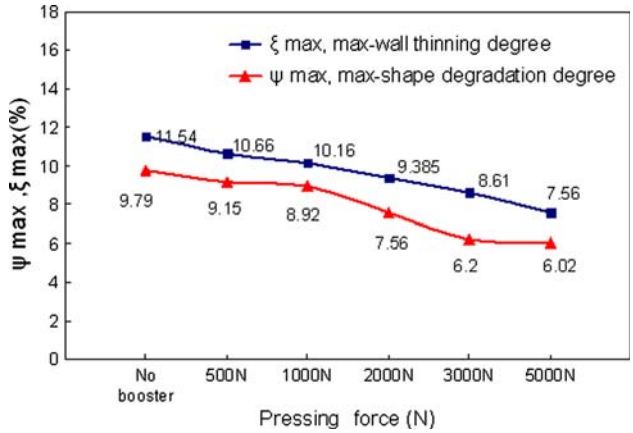

Fig. 20 Comparison of quality parameters under different pressing forces

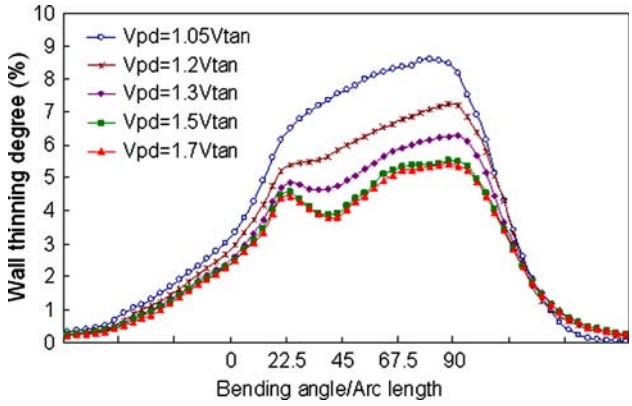

Fig. 21 Reduction of wall thickness at extrados

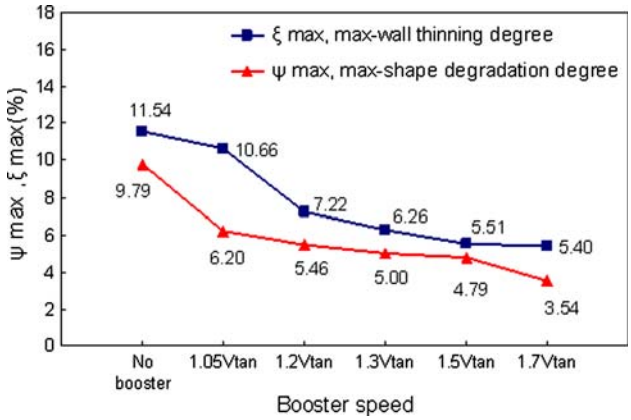

Fig. 22 Comparison of quality parameters under different booster speeds

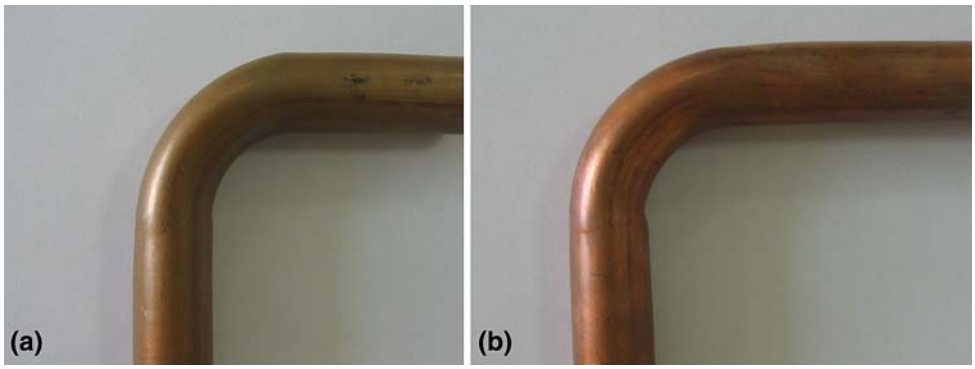

Fig. 23 Tube formed with different conditions: (a) without using booster system; (b) booster speed of $1.7V_{\tan}$ and pressure force of 1000 N

Figure 23 shows the finished quality of bent tubes at different processing conditions. When the booster speed is raised from $V_{\tan}$, the degradation of the sectional shape diminishes. As shown in Fig. 23(a), flattening of the section at the bending part is obvious. At the processing conditions of booster speed of $1.7V_{\tan}$ and pressing force of 1000 N the shape of the tube is very good, as shown in Fig. 23(b). It also proves that the booster system is able to improve effectively the forming quality of tube rotary draw bending.

5. Conclusions

In this study, the effect of surface booster system has been studied. Loading type was compared and a relationship between pressing force, booster speed, and forming quality was obtained. Based on the above investigation, the following conclusions can be drawn:

(1) Of the two kinds of loading modes, the force loading derived from hydraulic driving equipment performs better than displacement loading derived from lead-screw driving equipment.
(2) Surface booster system alleviates the defects of both wall thinning and sectional shape degradation simultaneously. It is able to improve the metal flow condition of the bending part especially a the extrados side.
(3) The larger the pressing force is, the more advantageous it is for the tube to form. The relationship is nearly linear. Pressing force between 1000 and 3000 N is the preferable range for bending of C12200 copper tube with a diameter of 20 mm, which is widely used in HVAC industry.
(4) The larger the booster speed is, the more advantageous it is for the tube to bend. The relationship is exponential descent, and $1.05V_{\tan}$ to $1.2V_{\tan}$ is the preferable range for booster speed.

The present research provides better understanding of the role of surface booster system in improvement of forming limit and forming quality. Design of processing parameters of the booster system is also guided.

Acknowledgments

The authors acknowledge the financial support of National Basic Pre-Research Program of China (2006CB708611), National Natural Science Foundation (No. 50634010), Shanghai Rising Star Project (06QA14026), Shanghai Science & Technology Projects (05JC14022).

References

1. F. Stachowicz, Bending with Upsetting of Copper Tube Elbows, *J. Mater. Process. Technol.*, 2000, **100**, p 236–240 (in English)
2. H. Lee, C.J. Van Tyne, and D. Field, Finite Element Bending Analysis of Oval Tubes Using Rotary Draw Bender for Hydroforming Applications, *J. Mater. Process. Technol.*, 2005, **168**, p 327–335 (in English)
3. H. Lou and K.A. Stelson, Three-Dimensional Tube Geometry Control for Rotary Draw Tube Bending. Part 1. Bend Angle and Overall Tube Geometry Control, *J. Manuf. Sci. Eng.*, 2001, **123**, p 258–265 (in English)
4. S.R. Reid, T.X. Yu, and I.L. Yang, Hardening-Softening Behaviour of Circular Pipes Under Bending and Tension, *Int. J. Mech. Sci.*, 1994, **36**, p 1073–1083 (in English)
5. H. Li, H. Yang, M. Zhan, Z. Sun, and R. Gu, Role of Mandrel in NC Precision Bending Process of Thin-Walled Tube, *Int. J. Mach. Tools Manuf.*, 2007, **7**, p 1164–1175 (in English)
6. Y. Peng, D. Tang, and D. Li, Study on the Influence of Mandrel Type on Copper Tube Rotary Draw Bending, *Int. J. Mater. Prod. Technol.*, accepted in Jun 2007 (in English)